

## **Implementation of 3-field model into TRAC**

**Sang-Ik Lee, Hee Cheon NO**

Korea Advanced Institute of Science and Technology  
373-1, Kusong-Dong, Yusong-Gu, Taejon, 305-701, Korea

### **ABSTRACT**

*TRAC-PF1 is modified to include the 3-field governing equations and physical model related to the droplet field. In deriving the present 3-field model, the droplet equation of motion used in the study of Varone and Rohsenow is used to calculate the relative velocity of the droplet and gas. The governing equations and physical models related to the droplet field are based on the 3-field model of COBRA-TF and the finite difference equations of these modified governing equations are derived in the form of TRAC-PF1. New solution matrix elements are derived and these are adopted to the solution step of TRAC-PF1.*

*The simulation results by the modified code are compared with these from Ishii's equilibrium entrainment correlation. It is found out that the simulation results depend on inlet void fraction and pipe diameter. When inlet void fraction is 0.9 or higher and the pipe diameter is larger than 3cm, the simulation results approach Ishii's correlation.*

### **1. INTRODUCTION**

The droplet entrained from a liquid film by a gas flow is important for heat and mass transfer processes in annular or annular-mist flow regime because the existence of droplets can significantly change the mechanisms of mass, momentum, and energy transfer between the film and the gas flow. It is also important because annular flow regime exists before dryout. In a nuclear reactor safety analysis, dryout is an important parameter because the heat transfer coefficient drops dramatically to bring a sudden increase in surface temperature at that point.

The essential features of annular flow regime are a liquid film flowing on the channel wall and a vapor core containing entrained droplets. These droplets are continually torn off the film, mainly due to large disturbance waves on the liquid film, and partly redeposited onto the film again.

TRAC is an advanced best-estimate systems code for analyzing LWR accidents. In this code, two-phase mixture is treated as a separated two-fluid with the two-field model. The two-field model has no consideration of droplets so the droplet velocity and the droplet size, which have important information about annular flow, are

calculated by empirical correlations.

On the other hand, COBRA, a core calculation code, treats two-fluid as separated three-field (gas, liquid film, droplet) to calculate complicated flow motions of core. COBRA better estimates than TRAC in case of Large Break Loss of Coolant Accident. Therefore, to accurately predict many important physical phenomena in droplet-annular flow, application of three-field model is needed.

## 2. PREVIOUS WORKS

### 2.1 Three-field models

In annular, or annular-mist flow regime, two-phase fluid must be treated as three flow field, because of interactions between liquid droplet and other fields (gas, liquid film). These interactions are considered by addition of droplet field in governing equations and the number of governing equations can be reduced by reasonable assumptions.

Two assumptions were made in using three-field model of COBRA-TF: The density and internal energies of liquid film and droplets are the same, respectively. [2]

Another three-field model is used in MONA code. [6] MONA has been designed as a general simulator for single component two-phase flow systems. It contains a set of seven conservation equations, based on the modeling of three flow fields. Assuming that the droplet field is moving at approximately the gas velocity, the momentum conservation equations for the gas phase and the droplets were added, yielding a combined momentum equation where the gas-droplet drag term is canceled out. The droplet velocity,  $V_d$ , is specified by an algebraic relation, relative to the gas velocity. Thus only two momentum equations are solved, one for the combined gas/droplet field and another for the continuous liquid field. For energy conservation, the liquid film and the droplet fields are assumed to be at the same temperature, and only two energy equations are used.

### 2.2 Varone-Rohsenow model

The Varone-Rohsenow model is an iterative method to estimate the heat transfer coefficient at post-dryout flow regime. It treats the major forces acting on droplets. In this model, only two-field was considered; liquid droplet and gas field. Several assumptions are made in this model.

1. vertical upflow in a circular tube.
2. uniform wall heat flux,
3. steady state conditions.
4. equilibrium quality exists at dryout,
5. both liquid and vapor are at the saturation temperature at dryout,
6. drop size distribution can be characterized by one average drop size,
7. liquid temperature remains at the saturation temperature.

The equation of motion used in this model is as follows.

$$M_d \frac{dV_d}{dt} = F_D - F_G,$$
$$F_D = \frac{1}{2} \left( \frac{\rho}{4} d^2 \right) C_D \mathbf{r}_g (V_g - V_d)^2,$$

$$F_G = \frac{\rho}{6} d^3 D r_g,$$

$$\frac{dV_d}{dt} = \frac{3C_D \mathbf{r}_g (V_g - V_d)^2}{4d \mathbf{r}_f} - \left(1 - \frac{\mathbf{r}_g}{\mathbf{r}_f}\right) g.$$

### 2.3 Empirical Correlations

Even though the three-field model is used, empirical correlations are needed in calculating the entrainment rate. The entrainment rate is an important factor which governs the quantity of entrainment. In the present work, several empirical correlations are used. [2],[4]

1. Mass fraction of evaporation of droplet field

$$\mathbf{h} : \begin{cases} \min \left[ \frac{g}{1-a}, \left(1.0 - \frac{q_{ev}}{\Gamma(h_f - h_g)}\right) \right], & \text{for vaporization} \\ \left( \frac{g}{1-a} \right), & \text{for condensation} \end{cases}$$

2. Entrainment rate (British Units)

Entrainment rates used in the present study are listed in Tables 2, 3 and 4.

3. Drag coefficient for droplet

$C_D$  : Varone-Rohsenow (Drag coefficient)

$$C_D = 27 / \text{Re}_d^{0.84} \quad \text{for } \text{Re}_d < 150 \quad \text{where } \text{Re}_d = \frac{(V_g - V_d) \mathbf{r}_g d}{\mathbf{m}_g}$$

$$C_D = 0.4 \quad \text{for } \text{Re}_d \geq 150$$

4. Droplet size

$d$  : droplet size and interfacial area

$$a_{g-d} = \frac{3.6 \mathbf{a}_d}{d} = 2.4 \frac{\mathbf{a}_d \mathbf{r}_g (V_g - V_f)^2}{\mathbf{s}} : \text{pre-CHF droplets}$$

5. Drag coefficient for droplet field

$C_{Dd}$  : droplet drag coefficient

$$C_{Dd} = \frac{24}{\text{Re}_d} \left(1.0 + 0.1 \text{Re}_d^{0.75}\right), \quad \begin{cases} \text{Re}_d = \frac{\mathbf{r}_g d |V_g - V_d|}{\mathbf{m}_b} \\ \mathbf{m}_b = \mathbf{m}_g \mathbf{a}_g^{-2.5} \frac{(\mathbf{m} + 0.4 \mathbf{m})}{(\mathbf{m}_v + \mathbf{m})} \end{cases}$$

## 3. NUMERICAL WORKS

### 3.1. Modified Governing Equations

First of all, governing equations must be changed in order to apply the three-field model. The governing equations of TRAC-PF1 is modified as follows:

Liquid Equation of Motion

$$\frac{\partial \bar{V}_l}{\partial t} + \bar{V}_l \cdot \nabla \bar{V}_l = -\frac{1}{\mathbf{r}_l} \nabla P + \frac{c_i}{(1-\mathbf{a}-\mathbf{g}) \mathbf{r}_l} (\bar{V}_g - \bar{V}_l) |\bar{V}_g - \bar{V}_l| - \frac{c_{wl}}{(1-\mathbf{a}-\mathbf{g}) \mathbf{r}_l} \bar{V}_l |\bar{V}_l| + \bar{g} + \frac{S(\bar{V}_l - \bar{V}_d)}{(1-\mathbf{a}-\mathbf{g}) \mathbf{r}_l}$$

Combined-Gas Equation of Motion

$$\frac{\partial \bar{V}_g}{\partial t} + \bar{V}_g \cdot \nabla \bar{V}_g = -\frac{1}{\mathbf{r}_g} \nabla P - \frac{c_i}{\mathbf{a} \mathbf{r}_g} (\bar{V}_g - \bar{V}_l) |\bar{V}_g - \bar{V}_l| - \frac{c_{wg}}{\mathbf{a} \mathbf{r}_g} \bar{V}_g |\bar{V}_g| - \frac{\mathbf{t}_{g-d}}{\mathbf{a} \mathbf{r}_g} + \bar{g}$$

Combined-Gas Mass Equation

$$\frac{\partial}{\partial t} \mathbf{a}_v \mathbf{r}_v + \nabla \cdot (\mathbf{a}_v \mathbf{r}_v U_v) = \Gamma''$$

Liquid mass Equation

$$\frac{\partial}{\partial t} \mathbf{a}_l \mathbf{r}_l + \nabla \cdot (\mathbf{a}_l \mathbf{r}_l U_l) = -(1-\mathbf{h})\Gamma'' - S'''$$

Liquid droplet mass Equation

$$\frac{\partial}{\partial t} \mathbf{a}_d \mathbf{r}_d + \nabla \cdot (\mathbf{a}_d \mathbf{r}_d U_d) = \mathbf{h}\Gamma'' + S'''$$

Noncondensable-Gas Mass Equation

$$\frac{\partial (\mathbf{a}_a)}{\partial t} + \nabla \cdot (\mathbf{a}_a \bar{V}_g) = 0$$

Combined-Gas Energy Equation

$$\frac{\partial}{\partial t} (\mathbf{a}_v \mathbf{r}_v h_v) + \nabla \cdot (\mathbf{a}_v \mathbf{r}_v h_v U_v) = \Gamma'' h_g + q_{iv} + q_{wv}$$

Total Energy Equation

$$\frac{\partial}{\partial t} [\mathbf{a}_g \mathbf{r}_g h_g + (\mathbf{a}_l + \mathbf{g}) \mathbf{r}_l h_l] + \nabla \cdot (\mathbf{a}_g \mathbf{r}_g h_g U_g) + \nabla \cdot (\mathbf{a}_l \mathbf{r}_l h_l U_l) + \nabla \cdot (\mathbf{g}_l h_l U_d) = \tilde{q}_{wg} + \tilde{q}_{wl}$$

Gas-droplet shear stress is added in gas momentum equation, and entrainment rate is added in liquid film momentum equation. Droplet mass equation is added in mass equation and evaporation rate is considered. Droplet energy equation and other field energy equation are added and the result is total energy equation.

## 3.2. Modified Finite Difference Equations

### 3.2.1. Momentum equations

First, momentum equations must be solved for new time velocities, with respect to pressure. In TRAC-PF1/MOD1, there are no effects of evaporation. For simplification, several assumptions are made in the droplet equation of motion. The assumptions used here are as follows.

1. Droplets are very small in size so the pressure drops in droplet fields are neglected
2. Momentum exchanges between droplet and liquid field are neglected.
3. The only effect of droplets in the momentum equation is the interfacial drag between gas and droplet fields.

These assumptions may be somewhat impractical but the whole aspects of flow will be maintained. The combined gas equation is as follows:

Combined gas

$$\begin{aligned} & \frac{(V_g^{n+1} - V_g^n)}{\Delta t} + V_g^n \nabla_{j+\frac{1}{2}} \tilde{V}_g^{n+1} + \mathbf{b} (V_g^{n+1} - V_g^n) \nabla_{j+\frac{1}{2}} \tilde{V}_g^n + \frac{c_i^n}{(\bar{\mathbf{a}}_g^n)_{j+\frac{1}{2}}} [2(V_g^{n+1} - V_l^{n+1}) - (V_g^n - V_l^n)] |V_g^n - V_l^n| \\ & + \frac{1}{(\bar{\mathbf{r}}_g^n)_{j+\frac{1}{2}}} \frac{(\tilde{p}_{j+1}^{n+1} - \tilde{p}_j^n)}{\Delta X_{j+\frac{1}{2}}} + \frac{c_{wg}}{(\bar{\mathbf{a}}_g^n)_{j+\frac{1}{2}}} (2V_g^{n+1} - V_g^n) |V_g^n| + \frac{(\mathbf{t}_{d-g})_{j+\frac{1}{2}}^{n+1}}{(\bar{\mathbf{a}}_g^n)_{j+\frac{1}{2}}} + g \cos \mathbf{q} = 0 \quad (3.1) \end{aligned}$$

$$\text{where } \mathbf{b} = \begin{cases} 0, & \text{if } \nabla_{j+\frac{1}{2}} V^n \leq 0 \\ 0, & \text{if } \nabla_{j+\frac{1}{2}} V^n < 0 \end{cases}$$

The droplet shear contribution term is presented in equation (3.1) and this term is represented by equation (3.2).

$$\left( \frac{\mathbf{t}_{g-d}}{\bar{\mathbf{a}}_g} \right)_{j+\frac{1}{2}}^{n+1} = \frac{K_{lge}^n V_{gd}^{n+1}}{(\bar{\mathbf{a}}_g^n)_{j+\frac{1}{2}}} = \frac{(0.375 \frac{C_{Db}}{b} \mathbf{a}_e \mathbf{r}_g)_{j+\frac{1}{2}}^n |V_{gd}^n| |V_{gd}^{n+1}|}{(\bar{\mathbf{a}}_g^n)_{j+\frac{1}{2}}} \quad (3.2)$$

$$\text{where } C_{Db} = \frac{24}{\text{Re}_D} (1.0 + 0.1 \cdot \text{Re}_D^{0.75}) ; \text{ Based on flow regime}$$

Equation (3.2) needs  $V_g$ - $V_d$  relationship. This term was derived from Varone-Rohsenow equation of motion.

The force balance equation of droplet is as follows;

$$M_d \frac{dV_d}{dt} = F_D - F_G,$$

$$F_D = \frac{1}{2} \left( \frac{\mathbf{p}}{4} d^2 \right) C_D \mathbf{r}_g (V_g - V_d)^2,$$

$$F_G = \frac{\rho}{6} d^3 \mathbf{D} r_g,$$

Basically, the Lagrangian description method is used in the Varone-Rohsenow equation of motion. In the Varone-Rohsenow equation of motion, only gravity and drag forces are in consideration. Other terms such as pressure gradient, virtual mass and Basset term, are neglected. This assumption is quite reasonable because they are of the order of gas/droplet density ratio. Varone-Rohsenow equation of motion is changed to Eulerian description method using definition of total derivative.

$$\frac{dV_d}{dt} = \frac{\partial V_d}{\partial t} + V_d \cdot \nabla V_d = \frac{3C_D \mathbf{r}_g (V_g - V_d)^2}{4d \mathbf{r}_f} - \left( 1 - \frac{\mathbf{r}_g}{\mathbf{r}_f} \right) g$$

$$\frac{V_d^{n+1} - V_d^n}{\Delta t} + V_d^n \cdot \nabla V_d^n = \left( \frac{3C_D \mathbf{r}_g}{4d \mathbf{r}_f} \right) |V_g^n - V_d^n| (V_g^{n+1} - V_d^{n+1}) - \left( 1 - \frac{\mathbf{r}_g}{\mathbf{r}_f} \right) g$$

$$\begin{aligned}
V_g^{n+1} - V_d^{n+1} &= \frac{1}{\left\{ 1 + \frac{\Delta t C_D^n}{4d^n} \left( \frac{r_g}{r_f} \right)^n |V_g^n - V_d^n| \right\}} V_g^{n+1} - \frac{1}{\left\{ 1 + \frac{\Delta t C_D^n}{4d^n} \left( \frac{r_g}{r_f} \right)^n |V_g^n - V_d^n| \right\}} V_d^n \\
&+ \frac{\frac{\Delta t C_D^n}{8d^n} \left( \frac{r_g}{r_f} \right)^n}{\left\{ 1 + \frac{\Delta t C_D^n}{4d^n} \left( \frac{r_g}{r_f} \right)^n |V_g^n - V_d^n| \right\}} |V_g^n - V_d^n| \left( V_g^n - V_d^n \right) + \frac{\frac{\Delta t}{6} \left( 1 - \frac{r_g}{r_f} \right) g \cos \mathbf{q}}{\left\{ 1 + \frac{\Delta t C_D^n}{4d^n} \left( \frac{r_g}{r_f} \right)^n |V_g^n - V_d^n| \right\}} \\
&+ \frac{V_d^n \nabla_{j+1/2} V_d^n \Delta t}{\left\{ 1 + \frac{\Delta t C_D^n}{4d^n} \left( \frac{r_g}{r_f} \right)^n |V_g^n - V_d^n| \right\}} \\
&= k_1^n V_g^{n+1} + k_2^n \quad (3.3)
\end{aligned}$$

where

$$\left\{ \begin{aligned}
k_1^n &= \frac{1}{\left\{ 1 + \frac{\Delta t C_D^n}{4d^n} \left( \frac{r_g}{r_f} \right)^n |V_g^n - V_d^n| \right\}} \\
k_2^n &= -\frac{1}{\left\{ 1 + \frac{\Delta t C_D^n}{4d^n} \left( \frac{r_g}{r_f} \right)^n |V_g^n - V_d^n| \right\}} V_d^n + \frac{\frac{\Delta t C_D^n}{8d^n} \left( \frac{r_g}{r_f} \right)^n}{\left\{ 1 + \frac{\Delta t C_D^n}{4d^n} \left( \frac{r_g}{r_f} \right)^n |V_g^n - V_d^n| \right\}} |V_g^n - V_d^n| \left( V_g^n - V_d^n \right) \\
&+ \frac{\frac{\Delta t}{6} \left( 1 - \frac{r_g}{r_f} \right) g \cos \mathbf{q}}{\left\{ 1 + \frac{\Delta t C_D^n}{4d^n} \left( \frac{r_g}{r_f} \right)^n |V_g^n - V_d^n| \right\}} + \frac{V_d^n \nabla_{j+1/2} V_d^n \Delta t}{\left\{ 1 + \frac{\Delta t C_D^n}{4d^n} \left( \frac{r_g}{r_f} \right)^n |V_g^n - V_d^n| \right\}}
\end{aligned} \right.$$

Equation (3.1) becomes

$$\begin{aligned}
&\frac{(V_g^{n+1} - V_g^n)}{\Delta t} + V_g^n \nabla_{j+\mathcal{Y}_2} \tilde{V}_g^{n+1} + \mathbf{b}(V_g^{n+1} - V_g^n) \nabla_{j+\mathcal{Y}_2} \tilde{V}_g^n + \frac{c_i^n}{(\bar{\mathbf{a}}_g)_{j+\mathcal{Y}_2}^n} \left[ 2(V_g^{n+1} - V_l^{n+1}) - (V_g^n - V_l^n) \right] |V_g^n - V_l^n| \\
&+ \frac{1}{(\bar{\mathbf{r}}_g)_{j+\mathcal{Y}_2}^n} \frac{(\tilde{p}_{j+1}^{n+1} - \tilde{p}_j^n)}{\Delta X_{j+\mathcal{Y}_2}} + \frac{(1-\mathbf{h})^n \Gamma_{j+\mathcal{Y}_2}^{n+1}}{(\bar{\mathbf{a}}_g)_{j+\mathcal{Y}_2}^n} (V_g^{n+1} - V_l^{n+1}) + \frac{\mathbf{h}^n \Gamma_{j+\mathcal{Y}_2}^n}{(\bar{\mathbf{a}}_g)_{j+\mathcal{Y}_2}^n} (k_1^n V_g^{n+1} + k_2^n) \\
&+ \frac{c_{wg}}{(\bar{\mathbf{a}}_g)_{j+\mathcal{Y}_2}^n} (2V_g^{n+1} - V_g^n) |V_g^n| + \frac{K_{lge}^n (k_1^n V_g^{n+1} + k_2^n)}{(\bar{\mathbf{a}}_g)_{j+\mathcal{Y}_2}^n} + g \cos \mathbf{q} = 0 \quad (3.4)
\end{aligned}$$

Liquid Equation of motion is presented and the momentum exchanges between liquid film and droplets are considered. in equation (3.5).

Liquid

$$\begin{aligned}
&\frac{(V_l^{n+1} - V_l^n)}{\Delta t} + V_l^n \nabla_{j+\mathcal{Y}_2} \tilde{V}_l^{n+1} + \mathbf{b}(V_l^{n+1} - V_l^n) \nabla_{j+\mathcal{Y}_2} \tilde{V}_l^n \\
&+ \frac{c_i^n}{\left[ (1-\mathbf{a}-\mathbf{g}) \bar{\mathbf{r}}_l \right]_{j+\mathcal{Y}_2}^n} \left[ 2(V_l^{n+1} - V_g^{n+1}) - (V_l^n - V_g^n) \right] |V_l^n - V_g^n|
\end{aligned}$$

$$\begin{aligned}
& + \frac{1}{(\bar{\rho}_l)^n} \frac{(\bar{p}_{j+1}^{n+1} - \bar{p}_j^n)}{\Delta X_{j+\frac{1}{2}}} - \frac{(1-\eta)\Gamma_{j+\frac{1}{2}}^n}{[(1-\alpha-\gamma)\bar{\rho}_l]_{j+\frac{1}{2}}^n} (V_l^{n+1} - V_g^{n+1}) - \frac{S^n (V_l^{n+1} - V_d^{n+1})}{[(1-\alpha-\gamma)\bar{\rho}_l]_{j+\frac{1}{2}}^n} \\
& + \frac{c_{wl}}{[(1-\alpha-\gamma)\bar{\rho}_l]_{j+\frac{1}{2}}^n} (2V_l^{n+1} - V_l^n) |V_l^n| + g \cos \theta = 0 \quad (3.5)
\end{aligned}$$

Equation (3.5) becomes equation (3.6) by substituting  $V_d$  as a function of  $V_g$  using equation (3.3) :

$$\begin{aligned}
& \frac{(V_l^{n+1} - V_l^n)}{\Delta t} + V_l^n \nabla_{j+\frac{1}{2}} \bar{V}_l^{n+1} + \beta (V_l^{n+1} - V_l^n) \nabla_{j+\frac{1}{2}} \bar{V}_l^n \\
& + \frac{c_l^n}{[(1-\alpha-\gamma)\bar{\rho}_l]_{j+\frac{1}{2}}^n} [2(V_l^{n+1} - V_g^{n+1}) - (V_l^n - V_g^n)] |V_l^n - V_g^n| \\
& + \frac{1}{(\bar{\rho}_l)^n} \frac{(\bar{p}_{j+1}^{n+1} - \bar{p}_j^n)}{\Delta X_{j+\frac{1}{2}}} - \frac{(1-\eta)\Gamma_{j+\frac{1}{2}}^n}{[(1-\alpha-\gamma)\bar{\rho}_l]_{j+\frac{1}{2}}^n} (V_l^{n+1} - V_g^{n+1}) - \frac{S^n (V_l^{n+1} - V_g^{n+1})}{[(1-\alpha-\gamma)\bar{\rho}_l]_{j+\frac{1}{2}}^n} \\
& - \frac{S^n (k_1^n V_g^{n+1} + k_2^n)}{[(1-\alpha-\gamma)\bar{\rho}_l]_{j+\frac{1}{2}}^n} + \frac{c_{wl}}{[(1-\alpha-\gamma)\bar{\rho}_l]_{j+\frac{1}{2}}^n} (2V_l^{n+1} - V_l^n) |V_l^n| + g \cos \theta = 0 \quad (3.6)
\end{aligned}$$

Two equations, (3.4) and (3.6), have two variables  $V_g$  and  $V_l$ , which are dependent on new time variable  $P^{n+1}$ . In mass, and energy equations, pressure and velocities are needed in calculating the primary variables  $P$ ,  $\alpha$ ,  $T_b$ ,  $T_l$ ,  $\gamma$ ,  $P_a$ . But in equations, (3.4) and (3.6),  $V_g$  and  $V_l$  are coupled, so this must be solved using 2x2 matrix inversion.

Combined-Gas Equation of Motion

$$\begin{aligned}
& \left( 1 + \Delta t \beta \nabla_{j+\frac{1}{2}} \bar{V}_g^n + \Delta t \frac{2c_l^n |V_g^n - V_l^n|}{(\alpha \rho_g)^n} + \frac{\Delta t (1-\eta) \Gamma_{j+\frac{1}{2}}^n}{(\alpha \rho_g)^n} + \frac{2\Delta t c_{wg}}{(\alpha \rho_g)^n} |V_g^n| + \frac{\Delta t \eta^n \Gamma_{j+\frac{1}{2}}^n k_1^n}{(\alpha \rho_g)^n} + \frac{\Delta t K_{Igs}^n k_1^n}{(\alpha \rho_g)^n} \right) V_g^{n+1} \\
& = V_g^n - \Delta t V_g^n \nabla_{j+\frac{1}{2}} \bar{V}_g^{n+1} + \Delta t \beta V_g^n \nabla_{j+\frac{1}{2}} \bar{V}_g^n - \Delta t \frac{c_l^n |V_g^n - V_l^n|}{(\alpha \rho_g)^n} [-2V_l^{n+1} - (V_g^n - V_l^n)] \\
& - \Delta t \frac{(P_{j+1}^{n+1} - P_j^{n+1})}{(\rho_g)^n \Delta x_{j+\frac{1}{2}}} + \frac{\Delta t (1-\eta) \Gamma_{j+\frac{1}{2}}^n V_l^{n+1}}{(\alpha \rho_g)^n} + \frac{\Delta t c_{wg}}{(\alpha \rho_g)^n} V_g^n |V_g^n| - \frac{\Delta t \eta^n \Gamma_{j+\frac{1}{2}}^n k_2^n}{(\alpha \rho_g)^n} - \frac{\Delta t K_{Igs}^n k_2^n}{(\alpha \rho_g)^n} - \Delta t g \cos \theta \quad (3.7)
\end{aligned}$$

Liquid Equation of Motion

$$\left( 1 + \Delta t \beta \nabla_{j+\frac{1}{2}} \bar{V}_l^{n+1} + \Delta t \frac{2c_l^n |V_l^n - V_g^n|}{[(1-\alpha-\gamma)\rho_l]_{j+\frac{1}{2}}^n} - \frac{\Delta t (1-\eta) \Gamma_{j+\frac{1}{2}}^n}{[(1-\alpha-\gamma)\rho_l]_{j+\frac{1}{2}}^n} \right)$$

$$\begin{aligned}
& + \frac{2\Delta t c_{wl}}{[(1-\mathbf{a}-\mathbf{g})\mathbf{r}_l]_{j+\frac{1}{2}}^n} |V_l^n| - \frac{S^n \Delta t}{[(1-\mathbf{a}-\mathbf{g})\mathbf{r}_l]_{j+\frac{1}{2}}^n} \Bigg) V_l^{n+1} \\
& = V_l^n - \Delta t V_l^n \nabla_{j+\frac{1}{2}} \tilde{V}_l^{n+1} + \Delta t \mathbf{b} V_l^n \nabla_{j+\frac{1}{2}} \tilde{V}_l^n - \Delta t \frac{c_i^n |V_l^n - V_g^n|}{[(1-\mathbf{a}-\mathbf{g})\mathbf{r}_l]_{j+\frac{1}{2}}^n} (-2V_g^{n+1} - (V_l^n - V_g^n)) \\
& - \Delta t \frac{(\tilde{P}_{j+1}^{n+1} - \tilde{P}_j^{n+1})}{(\mathbf{r}_l)_{j+\frac{1}{2}}^n \Delta x_{j+\frac{1}{2}}} - \frac{\Delta t (1-\mathbf{h}) \Gamma_{j+\frac{1}{2}}^{-n} V_g^{n+1}}{[(1-\mathbf{a}-\mathbf{g})\mathbf{r}_l]_{j+\frac{1}{2}}^n} + \frac{\Delta t S^n (k_1^n - 1) V_g^{n+1}}{[(1-\mathbf{a}-\mathbf{g})\mathbf{r}_l]_{j+\frac{1}{2}}^n} + \frac{\Delta t S^n (k_2^n)}{[(1-\mathbf{a}-\mathbf{g})\mathbf{r}_l]_{j+\frac{1}{2}}^n} \\
& + \frac{\Delta t c_{wl}}{[(1-\mathbf{a}-\mathbf{g})\mathbf{r}_l]_{j+\frac{1}{2}}^n} V_l^n |V_l^n| - \Delta t g \cos \mathbf{q} \quad (3.8)
\end{aligned}$$

Two equations have the form as follows:

$$C_{g1} V_g^{n+1} = C_{g2} V_l^{n+1} + C_{g3}$$

$$C_{l1} V_l^{n+1} = C_{l2} V_g^{n+1} + C_{l3}$$

$$C_{g1} = \left( 1 + \Delta t \mathbf{b} \nabla_{j+\frac{1}{2}} \tilde{V}_g^n + \Delta t \frac{2c_i^n |V_g^n - V_l^n|}{(\mathbf{a}\mathbf{r}_g)_{j+\frac{1}{2}}^n} + \frac{\Delta t (1-\mathbf{h}) \Gamma_{j+\frac{1}{2}}^{-n}}{(\mathbf{a}\mathbf{r}_g)_{j+\frac{1}{2}}^n} + \frac{2\Delta t c_{wg}}{(\mathbf{a}\mathbf{r}_g)_{j+\frac{1}{2}}^n} |V_g^n| + \frac{\Delta t \mathbf{h} \Gamma_{j+\frac{1}{2}}^{-n} k_1^n}{(\mathbf{a}\mathbf{r}_g)_{j+\frac{1}{2}}^n} + \frac{\Delta t K_{lge, j+\frac{1}{2}} k_1^n}{(\mathbf{a}\mathbf{r}_g)_{j+\frac{1}{2}}^n} \right)$$

$$C_{g2} = \Delta t \frac{2c_i^n |V_g^n - V_l^n|}{(\mathbf{a}\mathbf{r}_g)_{j+\frac{1}{2}}^n} + \frac{\Delta t (1-\mathbf{h}) \Gamma_{j+\frac{1}{2}}^{-n}}{(\mathbf{a}\mathbf{r}_g)_{j+\frac{1}{2}}^n}$$

$$\begin{aligned}
C_{g3} & = V_g^n - \Delta t V_g^n \nabla_{j+\frac{1}{2}} \tilde{V}_g^{n+1} + \Delta t \mathbf{b} V_g^n \nabla_{j+\frac{1}{2}} \tilde{V}_g^n + \Delta t \frac{c_i^n |V_g^n - V_l^n|}{(\mathbf{a}\mathbf{r}_g)_{j+\frac{1}{2}}^n} (V_g^n - V_l^n) - \Delta t \frac{(P_{j+1}^{n+1} - P_j^{n+1})}{(\mathbf{r}_g)_{j+\frac{1}{2}}^n \Delta x_{j+\frac{1}{2}}} + \frac{\Delta t c_{wg}}{(\mathbf{a}\mathbf{r}_g)_{j+\frac{1}{2}}^n} V_g^n |V_g^n| \\
& - \frac{\Delta t \mathbf{h} \Gamma_{j+\frac{1}{2}}^{-n} k_2^n}{(\mathbf{a}\mathbf{r}_g)_{j+\frac{1}{2}}^n} - \frac{\Delta t K_{lge, j+\frac{1}{2}} k_2^n}{(\mathbf{a}\mathbf{r}_g)_{j+\frac{1}{2}}^n} - \Delta t g \cos \mathbf{q}
\end{aligned}$$

$$C_{l1} = \left( 1 + \Delta t \mathbf{b} \nabla_{j+\frac{1}{2}} \tilde{V}_l^{n+1} + \Delta t \frac{2c_i^n |V_l^n - V_g^n|}{[(1-\mathbf{a}-\mathbf{g})\mathbf{r}_l]_{j+\frac{1}{2}}^n} - \frac{\Delta t (1-\mathbf{h}) \Gamma_{j+\frac{1}{2}}^{-n}}{[(1-\mathbf{a}-\mathbf{g})\mathbf{r}_l]_{j+\frac{1}{2}}^n} \right)$$

$$+ \frac{2\Delta t c_{wl}}{[(1-\mathbf{a}-\mathbf{g})\mathbf{r}_l]_{j+\frac{1}{2}}^n} |V_l^n| - \frac{S^n \Delta t}{[(1-\mathbf{a}-\mathbf{g})\mathbf{r}_l]_{j+\frac{1}{2}}^n}$$

$$C_{l2} = \Delta t \frac{2c_i^n |V_l^n - V_g^n|}{[(1-\mathbf{a}-\mathbf{g})\mathbf{r}_l]_{j+\frac{1}{2}}^n} - \frac{\Delta t (1-\mathbf{h}) \Gamma_{j+\frac{1}{2}}^{-n}}{[(1-\mathbf{a}-\mathbf{g})\mathbf{r}_l]_{j+\frac{1}{2}}^n} + \frac{\Delta t S^n (k_1^n - 1)}{[(1-\mathbf{a}-\mathbf{g})\mathbf{r}_l]_{j+\frac{1}{2}}^n}$$

$$C_{l3} = V_l^n - \Delta t V_l^n \nabla_{j+\frac{1}{2}} \tilde{V}_l^{n+1} + \Delta t \mathbf{b} V_l^n \nabla_{j+\frac{1}{2}} \tilde{V}_l^n - \Delta t \frac{c_i^n |V_l^n - V_g^n|}{[(1-\mathbf{a}-\mathbf{g})\mathbf{r}_l]_{j+\frac{1}{2}}^n} (V_l^n - V_g^n)$$



$$-\Delta t \frac{(\bar{p}_{j+1}^{n+1} - \bar{p}_j^{n+1})}{(\rho_l)_{j+\frac{1}{2}}^n \Delta x_{j+\frac{1}{2}}} + \frac{\Delta t S^n (k_2^n)}{[(1-\alpha-\gamma)\rho_l]_{j+\frac{1}{2}}^n} + \frac{\Delta t c_{wl}}{[(1-\alpha-\gamma)\rho_l]_{j+\frac{1}{2}}^n} V_l^n |V_l^n| - \Delta t g \cos \theta$$

Solving linear systems with these form yields

$$C_{g1} V_g^{n+1} = C_{g2} V_l^{n+1} + C_{g3}$$

$$C_{l1} V_l^{n+1} = C_{l2} V_g^{n+1} + C_{l3}$$

$$\begin{pmatrix} C_{g1} & -C_{g2} \\ -C_{l1} & C_{l2} \end{pmatrix} \begin{pmatrix} V_g^{n+1} \\ V_l^{n+1} \end{pmatrix} = \begin{pmatrix} C_{g3} \\ C_{l3} \end{pmatrix}$$

$$\begin{pmatrix} V_g^{n+1} \\ V_l^{n+1} \end{pmatrix} = \frac{1}{C_{g1}C_{l1} - C_{g2}C_{l2}} \begin{pmatrix} C_{l1} & C_{g2} \\ C_{g1} & -C_{l2} \end{pmatrix} \begin{pmatrix} C_{g3} \\ C_{l3} \end{pmatrix} = \frac{1}{C_{g1}C_{l1} - C_{g2}C_{l2}} \begin{pmatrix} C_{l1}C_{g3} + C_{g2}C_{l3} \\ C_{g1}C_{l3} - C_{l2}C_{g3} \end{pmatrix}$$

After solving these two equations,

$$V_g^{n+1} = \frac{C_{l1}C_{g3} + C_{g2}C_{l3}}{C_{g1}C_{l1} - C_{g2}C_{l2}}, \quad V_l^{n+1} = \frac{C_{l2}C_{g3} + C_{g1}C_{l3}}{C_{g1}C_{l1} - C_{g2}C_{l2}}$$

$$\therefore \frac{dV_g^{n+1}}{d\bar{p}_{j+1}^{n+1}} = -\frac{\left( \frac{\Delta t}{C_{g2}\rho_{g,j+1/2}^n \Delta x_{j+1/2}} + \frac{\Delta t}{C_{l1}\rho_{l,j+1/2}^n \Delta x_{j+1/2}} \right)}{\left( \frac{C_{g1}}{C_{g2}} - \frac{C_{l2}}{C_{l1}} \right)} \quad \text{and} \quad \frac{dV_l^{n+1}}{d\bar{p}_{j+1}^{n+1}} = -\frac{dV_g^{n+1}}{d\bar{p}_{j+1}^{n+1}}$$

$$\therefore \frac{dV_l^{n+1}}{d\bar{p}_{j+1}^{n+1}} = -\frac{\left( \frac{\Delta t}{C_{l2}\rho_{l,j+1/2}^n \Delta x_{j+1/2}} + \frac{\Delta t}{C_{g1}\rho_{g,j+1/2}^n \Delta x_{j+1/2}} \right)}{\left( \frac{C_{l1}}{C_{l2}} - \frac{C_{g2}}{C_{g1}} \right)} \quad \text{and} \quad \frac{dV_g^{n+1}}{d\bar{p}_{j+1}^{n+1}} = -\frac{dV_l^{n+1}}{d\bar{p}_{j+1}^{n+1}}$$

### 3.2.2. Mass and Energy equations

The finite difference form of mass and energy equations are as follows.

Combined-Gas Mass Equation

$$\frac{[(\bar{\alpha}\bar{\rho}_g)^{n+1} - (\bar{\alpha}\bar{\rho}_g)^n]}{\Delta t} + \nabla_j \cdot (\alpha\rho_g V_g^{n+1}) = \bar{\Gamma}^{n+1}$$

Liquid mass Equation

$$\frac{[(1-\bar{\alpha}-\bar{\gamma})\bar{\rho}_l^{n+1} - (1-\bar{\alpha}-\bar{\gamma})\bar{\rho}_l^n]}{\Delta t} + \nabla_j \cdot [(1-\alpha-\gamma)\rho_l V_l^{n+1}] = -(1-\bar{\eta}^{n+1})\bar{\Gamma}^{n+1} - \bar{S}^{n+1}$$

Liquid droplet mass Equation

$$\frac{[(\bar{\gamma}\bar{\rho}_g)^{n+1} - (\bar{\gamma}\bar{\rho}_g)^n]}{\Delta t} + \nabla_j \cdot (\gamma\rho_g V_g^{n+1}) = -\bar{\eta}^{n+1}\bar{\Gamma}^{n+1} + \bar{S}^{n+1}$$

Noncondensable-Gas Mass Equation

$$\frac{[(\tilde{\mathbf{a}}_a)^{n+1} - (\tilde{\mathbf{a}}_a)^n]}{\Delta t} + \nabla_j \cdot (\mathbf{a}_a V_g^{n+1}) = 0$$

Combined-Gas Energy Equation

$$\frac{[(\tilde{\mathbf{a}}_g \tilde{e}_g)^{n+1} - (\mathbf{a}_g e_g)^n]}{\Delta t} + \nabla_j \cdot (\mathbf{a}_g e_g V_g^{n+1}) + \tilde{P}^{n+1} \left[ \frac{(\tilde{\mathbf{a}}^{n+1} - \mathbf{a}^n)}{\Delta t} + \nabla_j \cdot (\mathbf{a}^n V_g^{n+1}) \right] = \tilde{q}_{wg}^{n+1} + \tilde{q}_{ig}^{n+1} + \tilde{\Gamma}^{n+1} + \tilde{h}_{sg}^{n+1}$$

Combined Internal Energy Equation

$$\frac{[\tilde{\mathbf{a}}_g \tilde{e}_g + (1 - \tilde{\mathbf{a}}) \tilde{\mathbf{r}}_l \tilde{e}_l]^{n+1} - [\mathbf{a}_g e_g + (1 - \mathbf{a}) \mathbf{r}_l e_l]^n}{\Delta t} + \nabla_j \cdot [(\mathbf{a}_g e_g) V_g^{n+1} + (1 - \mathbf{a} - \mathbf{g}) \mathbf{r}_l e_l V_l^{n+1} + (\mathbf{g}_l e_l) V_d^{n+1}] + \tilde{P}^{n+1} \nabla_j \cdot [(1 - \mathbf{a} - \mathbf{g})^n V_l^{n+1} + \mathbf{a}^n V_v^{n+1} + \mathbf{g}^n V_d^{n+1}] = \tilde{q}_{wg}^{n+1} + \tilde{q}_{wl}^{n+1}$$

These finite difference equations are linearized by 6 primary variables,  $P$ ,  $\mathbf{a}$ ,  $T_g$ ,  $T_l$ ,  $\mathbf{g}$ ,  $P_a$ . And the solution matrix was derived.

## 4. RESULTS AND DISCUSSION

### 4.1 Application of 3-field models

After derivation of new solution matrix, the application to TRAC-PF1 is developed. As the original TRAC-PF1 is too complicated to do this work, simplified TRAC-PF1, named LANCELOT from KNFC (Korea Nuclear Fuel Company) is used.

LANCELOT is simplified for study of TRAC numerics, and complicated modules including heat transfer module were removed. The basic solution step of TRAC-PF1 is constructed of three subroutines named [tf1ds1], [tf1ds], [tf1ds3]. These are controlled by subroutine [tf1d]. [tf1ds1] is the subroutine for the basic momentum equation, [tf1ds] for the basic mass and energy equation, and [tf1ds3] is used to update variables used in this code. The 3-field model derived in chapter 3 is used to modify these subroutines and subroutine [tf1ds\_drop] is added to calculate the droplet velocity explicitly.

### 4.2 Test of code with simple geometry

Simple pipe geometry is considered in order to test results. Figure 1 shows the test code geometry. The flow boundary conditions specify the velocities of phases, and the pressure boundary conditions specify the pressure of the pipe exit. Comparison with experimental data are presented. Ishii (1989) developed empirical correlation of hydraulic equilibrium entrainment fraction. With the test geometry, entrainment fraction is assumed to be in equilibrium state in the 12<sup>th</sup> cell. With the initial conditions from Fig.7, transient calculations are performed during 55 seconds, and those results are assumed to be at steady-state. The calculation results are compared to Ishii's empirical correlation.

### 4.3 Results and Discussion

Figure 2 shows comparison of Ishii's equilibrium entrainment correlation [7] with experimental data at various experimental results. Ishii integrated various experimental results, and these results can be integrated to one correlation in log scale. Experimental data expressed with circles matches well with this correlation.

From Figure 3 to Figure 5, equilibrium entrainment correlation at various vapor velocities are plotted, and are compared with Ishii's correlation. The  $v_v$  is flow boundary gas velocity and initial pipe gas velocity. In the simulation test, flow boundary gas velocity and initial pipe gas velocity is same.

Figure 3 shows variation of simulation results as void fraction changes from 0.8 to 0.95, with fixed diameter at 1.5cm. The result is somewhat overestimating at low flow. But the overestimation becomes smaller and gets closer to Ishii's correlation as void fraction goes higher. Figures 4 and 5 show simulation results at different diameter and void fraction of 0.9. The simulation results approach Ishii's correlation as the diameter becomes larger. From Figures 3, 4, 5, in any cases, simulation results are somewhat higher than Ishii's correlation in low flow condition and lower in high flow condition. So we need to consider the rate of entrainment which is used in this study. In this present study, the entrainment correlations of COBRA-TF [2] were used. In view of these correlations two main factors which govern the amount of entrainment are in consideration. One is entrainment rate and the other is deentrainment rate. As described in Tables 2 and 3, the entrainment rate can vary with  $k_e$  and the deentrainment rate can vary with  $k_d$ . With this fact, sensitivity test about  $k_e$ ,  $k_d$  is in preparation.

## 5. CONCLUSIONS

The three-field model is developed and TRAC-PF1 is modified to be able to calculate entrainment volume fraction in the solution step. The tendency of results is the same as experimental works, but these are different in quantity when inlet void fraction and diameter of pipe is changed. From simulation results at various conditions, the following conclusions are obtained:

- 1) Inlet void fraction and diameter of pipe is important factors which govern entrainment fraction.
- 2) The simulation results for entrainment fraction approach the experimental data when pipe diameter is larger than 3 cm or initial void fraction is higher than 0.9.

From the present study, the followings are recommended as further works.

- 1) Entrainment rate correlation must be checked for various conditions.
- 2) The pressure gradient of the droplet field is neglected in this work for simplification, but this must be checked for transient calculation.

## NOMENCLATURE

### English

A	Area
c	Shear or friction coefficient in two-fluid equations
$c_p$	Specific heat at constant pressure
$c_v$	Specific heat at constant volume
D	Diameter
e	Specific internal energy
g	Gravitational acceleration
G	Mass flux

$h$	Specific enthalpy or heat-transfer coefficient
$h_{lg}$	Latent heat of vaporization
$P$	Pressure
$q$	Heat generation rate
$Re$	Reynolds number
$T$	Temperature
$V$	Velocity
$vol$	Hydraulic cell volume
$We$	Weber number

### **Greek**

$\alpha$	Vapor volume fraction
$\Gamma$	Net volumetric vapor-production rate caused by phase change
$\gamma$	Entrainment volume fraction
$\delta$	Film thickness
$\mu$	Viscosity
$\rho$	Density
$\sigma$	Surface tension
$\tau$	Shear stress
$\Delta$	Increment

### **Subscript**

$a$	Noncondensable gas
$d$	Droplet
$f$	Friction
$g$	Gas field or vapor
$i$	Interface
$j$	One-dimensional cell index in hydrodynamics equations
$l$	Liquid field
$m$	Mixture quantities
$s$	Saturation quantities
$v$	Water vapor (steam)

### **Superscript**

$k$	Iteration count index
$n, n+1$	Time-step boundary indices

## **REFERENCES**

- [1] "TRAC-PF1/MOD2 Vol 1. Theory Manual", NUREG/CR-5673 LA-12031-M, Vol. I
- [2] "COBRA/TRAC – A thermal-hydraulics code for transient analysis of nuclear reactor vessels and primary coolant systems", NUREG/CR-3046 PNL-4385, March, 1983
- [3] "TRAC-PF1: An advanced best-estimate computer program for pressurized water reactor analysis", NUREG/CR-3567 LA-9944-MS, February, 1984
- [4] "Relap5/MOD3 code manual Vol 4. Models and Correlations" pp. [4-7]-[4-9], NUREG/CR-5535 INEL-95/0174 Vol. 4, June, 1995
- [5] A. F. Varone, Jr. and W. M. Rohsenow, "Post dryout heat transfer prediction", Nuclear Engineering and Design 95 (1986) pp. 315-327
- [6] N. Hoyer, "Calculation of dryout and post-dryout heat transfer for tube geometry", Int. J. Multiphase Flow Vol. 24, No. 2, pp. 319-334, 1998
- [7] M. Ishii and K. Mishima, "Droplet entrainment correlation in annular two-phase flow", Int. J. Heat Mass Transfer. Vol. 32, No. 10, pp. 1835-1846, 1989
- [8] C. T. Crowe, M. P. Sharma, D. E. Stock, "The Particle-Source-In Cell Model for gas-droplet flows", Journal of Fluids Engineering, June 1977 [1] Banerjee, S., Chang, J-S., Girard, R., and Krishnan, V. S., "Reflux Condensation and Transition to Natural Circulation in a Vertical U-Tube," J. Heat Transfer, Vol. 105, pp. 719-727, 1983.

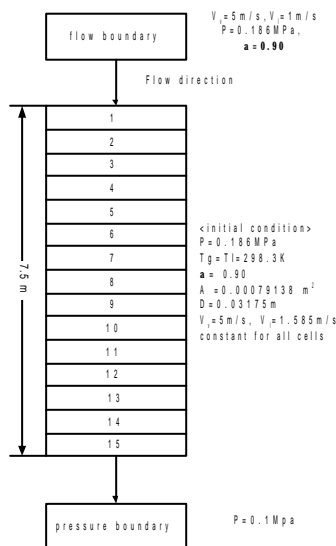


Figure 1. Test code geometry

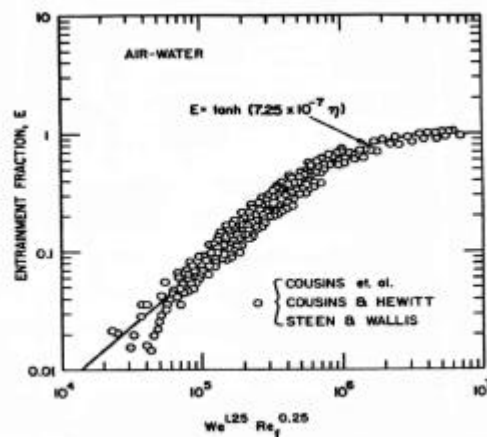


Figure 2. Comparison of equilibrium entrainment

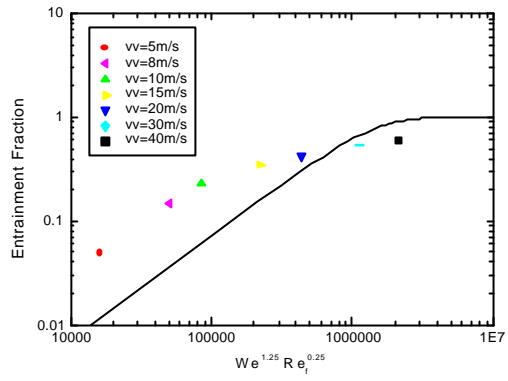
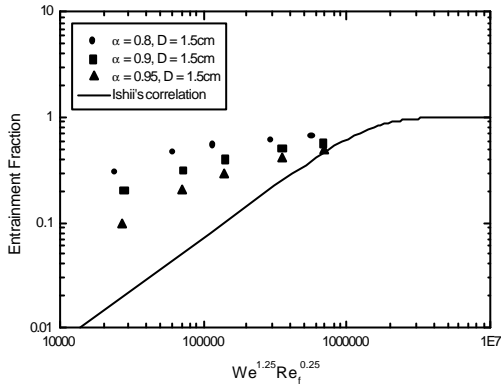


Figure 3. Simulation result at various void fraction Figure 4. Simulation result at D=3.175 cm, void 0.90

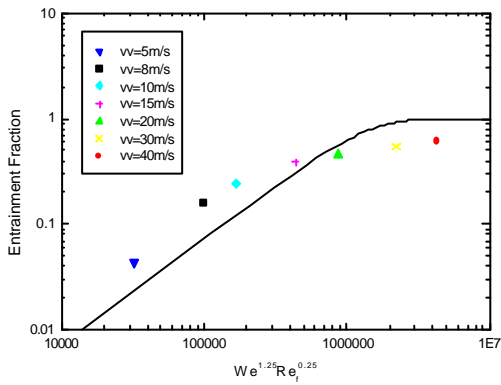


Figure 5. Simulation result at D=5 cm, void 0.90

Table 1. Test matrix of simulation test

Diameter	D=1.5 cm	D=3.75 cm	D=5 cm
Void fraction	$\alpha=0.80$	$\alpha=0.90$	$\alpha=0.95$

Table 2. Entrainment correlations at two different flow types

	Film, counter-current flow	Film, co-current flow
$S_E$	$(\alpha - \alpha_{crit}) r_l  V_l  A$	$0.41 S_u P_w \Delta x$
$S_{DE}$	$k_s \Delta C P_w \Delta x$	$k_s \Delta C P_w \Delta x$
$S$	$S_E - S_{DE}$	$S_E - S_{DE}$

**Table 3. Additional correlations for Table 2**

Counter-current $S_E$	Co-current $S_E$	$S_{DE}$
$\mathbf{a}_{crit} = \frac{4c_1 \mathbf{S}}{\mathbf{r}_g (V_g - V_l)^2 D_H}$	$S_u = \frac{k_s \mathbf{t}_l V_l \mathbf{m}_l}{\mathbf{S}^2}$	$k_s = \frac{1}{3.2808^4} \max\{3.0491 \times 10^{12} (\mathbf{S} \times 0.07562)^{5.3054}, 12.491 (\mathbf{S} \times 0.07562)^{0.8968}\}$
$\mathbf{a}_{g_{crit}} = 1 - \mathbf{a}_{l_{crit}} \geq 0.8$	$k_s = [0.57] \mathbf{d} + 2.1735 \times 10^4 \mathbf{d}^2 - 3.8319 \times 10^7 \mathbf{d}^3 + 5.5569 \times 10^{10} \mathbf{d}^4$	$\Delta C = \frac{\mathbf{a}_v \mathbf{r}_l}{\mathbf{a}_g + \mathbf{a}_v}$
$c_1 = 0.5$	$\mathbf{t}_l = \frac{f_l}{2} \mathbf{r}_g  V_{gl} ^2$	

**Table 4. Interfacial friction factor used in co-current flow**

Stable film flow; Wallis' s correlation	$f_l = 0.005 (1 + 75 \mathbf{a}_l)$
Unstable film flow; Henstock & Hanratty's correlation	$f_l = f_s \left\{ 1 + 1400 F \left[ 1 - \exp \left( - \frac{1}{G} \frac{(1 + 1400 F)^{3/2}}{13.2 F} \right) \right] \right\}$ $G = \frac{\mathbf{r}_g g D_H}{\mathbf{r}_g V_g^2 f_s}$ $F = \frac{m^+}{\text{Re}_g^{0.9}} \frac{\mathbf{m}_l}{\mathbf{m}_g} \sqrt{\frac{\mathbf{r}_g}{\mathbf{r}_l}}$ $m^+ = \left[ (0.707 \text{Re}_l^{0.5})^{2.5} + (0.0379 \text{Re}_l^{0.9})^{2.5} \right]^{0.40}$ $f_s = 0.046 \text{Re}_g^{-0.20}$